J. Biochem. **134**, 567–574 (2003)
DOI: 10.1093/jb/mvg175

Genetic, Enzymatic, and Structural Analyses of Phenylalanyl-tRNA Synthetase from *Thermococcus kodakaraensis* KOD1

Kentaro Shiraki[1], Masao Tsuji[2], Yoshiteru Hashimoto[3], Kenzo Fujimoto[1], Shinsuke Fujiwara[4], Masahiro Takagi[1] and Tadayuki Imanaka[*,5]

[1]School of Materials Science, Japan Advanced Institute of Science and Technology, 1-1 Asahidai, Tatsunokuchi, Ishikawa 923-1292; [2]Department of Biotechnology, Graduate School of Engineering, Osaka University, 2-1 Yamadaoka, Suita, Osaka 565-0871; [3]Institute of Applied Biochemistry, University of Tsukuba, 1-1-1 Tennodai, Tsukuba 305-8572; [4]Department of Bioscience, School of Science and Engineering, Kwansei-Gakuin University, 2-1 Gakuen Sanda, Hyogo 669-1337; and [5]Department of Synthetic Chemistry and Biological Chemistry, Graduate School of Engineering, Kyoto University, Nishikyo-ku, Kyoto 615-8510

Received May 14, 2003; accepted August 1, 2003

Phenylalanyl-tRNA synthetase from the hyperthermophilic archaeon *Thermococcus kodakaraensis* KOD1 (*Tk*-PheRS) was cloned. The open reading frames for both the α-subunit (*Tk-pheRSA*) and β-subunit (*Tk-pheRSB*) genes were 1,503 bp (501 amino acids) and 1,722 bp (574 amino acids), respectively. *Tk-pheRSB* located 879 bp downstream from *Tk-pheRSA* with a putative TATA box, suggesting that these two subunits are transcribed and regulated independently in KOD1 cells. *Tk*-PheRS and its respective subunits were expressed in *Escherichia coli* cells and the proteins were purified. *Tk*-PheRS showed an optimum enzymatic activity at around 95°C and retained its tertiary structure at 98°C. The estimated isoelectric point (p*I*) for the α-subunit is 9.4 and that for the β-subunit is 4.6, the largest difference among the 12 kinds of PheRSs reported. The considerable thermostability of *Tk*-PheRS may be responsible for the electrostatic interaction between the α- and β-subunits.

Key words: electrostatic interaction, heterooligomeric protein, hyperthermophilic protein, phenylalanyl-tRNA synthetase.

Abbreviations: aaRS, aminoacyl-tRNA synthetase; CAPS, *N*-cyclohexyl-3-aminopropanesulfonic acid; CD, circular dichroism; Da, Dalton; EDTA, ethylenediaminetetraacetic acid; FRET, fluorescence electron transfer; IPTG, isopropyl-β-D-thiogalactopyranoside; mdATP, *N*-methylanthranioyl deoxy ATP; HEPES, *N*-2-hydroxyethylpiperazine-*N*′-2-ethanesulfonic acid; PheRS, phenylalanyl-tRNA synthetase; PheRSA, α-subunit of PheRS; PheRSB, β-subunit of PheRS; SDS-PAGE, sodium dodecyl sulfate-polyacrylamide gel electrophoresis; *Tk*, *Thermococcus kodakaraensis* KOD1; Tris, 2-amino-2-hydroxymethyl-1,3-propanediol; UV, ultraviolet.

Aminoacyl-tRNA synthetases (aaRSs) play a central role in ensuring the fidelity of translation of the genetic code through selection of the correct amino acid (*1–4*). Every aaRS exerts restricted specificity for each respective amino acid. The aaRSs are generally divided into two classes by comparison of their primary structures, indicating that there are two evolutionary families of aaRSs (*5*). During the past decade, tertiary structures of 15 kinds of aaRSs, including TyrRS (*6*), GlnRS (*7*), MetRS (*8*), TrpRS (*9*), GluRS (*10*), IleRS (*11*), and ArgRS (*12*) in class I and SerRS (*13*), AspRS (*14*), LysRS (*15*), GlyRS (*16*), PheRS (*17*), ProRS (*18*), and AsnRS (*19*) in class II have been determined. Analyses of their structural properties and DNA sequences have revealed that most aaRSs have either a monomeric or homooligomeric structure, with the exception of several GlyRSs and PheRSs, which have $\alpha_2\beta_2$ heterooligomeric structure.

PheRS (phenylalanyl-tRNA synthetase; EC 6.1.1.20) is the largest and most complicated enzyme, with an $\alpha_2\beta_2$ heterotetrameric structure (*17*, *20–25*), classified as a class II enzyme on the basis of sequence motifs and protein folding. However, the enzymatic properties of PheRS are still unclear, because class I tRNA synthetases and PheRS charge the 2′-hydroxyl group of the tRNA acceptor stem while class II enzymes, except PheRS, charge the 3′-hydroxyl group of the tRNA acceptor stem. In addition, mitochondrial PheRS exhibits a monomeric form with similarity to the α-subunits of cytoplasmic PheRSs (*26*). Although it will be interesting to reveal both the enzymatic and structural properties of archaeal PheRS, to date only PheRSs from *Methanosarcina barkeri* (*27*) and *Methanobacterium thermoautotrophicum* (*28*) have been purified.

In this paper, we report the gene cloning and purification as well as enzymatic and structural analyses of an archaeal PheRS from *Thermococcus kodakaraensis* KOD1. *T. kodakaraensis* KOD1 is one of the most thermophilic organisms with an optimum growth temperature of 95°C (*29*) and full genome analysis is in progress. Previously, we reported the gene cloning and X-ray crystal structure analysis at 1.9 Å resolution of the AspRS protein from *T. kodakaraensis* KOD1 (*30–32*). This paper deals with the characterization of recombinant PheRS and the respective α (PheRSA) and β (PheRSB) subunits from *T. kodakaraensis* KOD1.

[*]To whom correspondence should be addressed. Tel: +81-75-383-2777, Fax: +81-75-383-2778, E-mail: imanaka@sbchem.kyoto-u.ac.jp

MATERIALS AND METHODS

Isolation and Sequencing of the pheRS Gene from T. kodakaraensis KOD1—In order to obtain the *pheRS* gene from KOD1 cells, PCR was carried out using primers designed on the basis of conserved amino acid sequences among PheRSs. The primers used were 5′-CA(C/T)CC(G/A)GC(A/G)(A/C)G(G/A)GA(C/A)ATGCA(G/A)GACAC(T/C)TT-3′ and 5′-GGCTC(A/G)GTGAA(C/T)GGGAAGTA-3′. An amplified 460-bp DNA fragment corresponding to part of the *Tk-pheRS* gene was obtained. The fragment was then used as a probe to isolate a phage clone that spanned the entire *Tk-pheRS* gene from the genomic DNA library of *T. kodakaraensis* KOD1 using the λEMBL4 phage vector. The selected phage DNA fragment was subcloned into pBluescript II SK+ (STRATAGENE, La Jolla, CAL) and the nucleotide sequence was determined using an ABI Model 310 capillary DNA sequencer PRISM with a dye-terminator sequencing kit (Perkin-Elmer Applied Biosystems, Foster City, CAL). For gene expression, *Tk-pheRSA* (α-subunit) and *Tk-pheRSB* (β-subunit) were respectively subcloned into pET-25b(+) (Novagen, Madison, WIS). The resultant plasmids were designated pET-*pheRSA* and pET-*pheRSB*, respectively. To express *Tk-pheRS* (both α- and β-subunits), the fragment harboring the T7 promoter and *Tk-pheRSB* gene derived from pET-*pheRSB* was inserted into pET-*pheRSA*. The resultant plasmid, designated pET-*pheRS*, carried both *Tk-pheRSA* and *Tk-pheRSB* located under the control of the T7 promoter.

Expression of Tk-PheRSA, Tk-PheRSB, and Tk-PheRS—The recombinant proteins were each overproduced in *E. coli* BL21-CodonPlus (DE3)-RIL (STRATAGENE) cells harboring the respective recombinant plasmids. When the optical density at 660 nm reached 0.4, expression was induced with 1 mM isopropyl-β-D-thiogalactopyranoside (IPTG) for 4 h. The cells from the culture broth (2.5 liters) were harvested by centrifugation and disrupted by sonication in 150 ml of 50 mM Tris-HCl buffer (pH 8.0) for *Tk*-PheRS or 20 mM Tris-HCl buffer (pH 9.0) for the recombinant α- and β-subunits. The supernatants were recovered after centrifugation at 15,000 ×*g* for 30 min at 4°C, and subjected to heat treatment at 80°C for 20 min. The samples were then centrifuged (20,000 ×*g*) at 4°C for 60 min and dialyzed overnight against 50 mM Tris-HCl buffer (pH 8.0) for *Tk*-PheRS or 20 mM Tris-HCl buffer (pH 9.0) for the α- and β-subunits.

Purification of Tk-PheRS—The dialyzed *Tk*-PheRS was applied to a HiTrap Heparin column (5 ml; Pharmacia Biotech, Uppsala, Sweden) equipped with an ÄKTA FPLC system (Pharmacia Biotech) at 4°C equilibrated with 50 mM Tris-HCl buffer (pH 8.0). The adsorbed fraction was eluted with 50 mM Tris-HCl buffer (pH 8.0) containing 1 M NaCl, and dialyzed overnight against 50 mM Tris-HCl buffer (pH 8.0) at 4°C. The sample was applied to a Mono Q column (1 ml; Pharmacia Biotech) equipped with the ÄKTA FPLC system at 4°C. The adsorbed fraction was eluted with a linear gradient consisting of 10 column volumes of 0 M to 1 M NaCl in 50 mM Tris-HCl buffer (pH 8.0). The purified solution was applied to a Superdex 200 HR column (24 ml; Pharmacia Biotech) equilibrated with 20 mM Tris-HCl buffer (pH 8.0) and 50 mM NaCl. The homogeneity of the purified protein was confirmed by SDS-PAGE.

Purification of the α-Subunit—The dialyzed α-subunit was applied to a HiTrap Q column (5 ml; Pharmacia Biotech) equipped with the ÄKTA FPLC system at 4°C equilibrated with 20 mM Tris-HCl buffer (pH 9.0). The non-adsorbed fraction was applied to a HiTrap SP column (5 ml; Pharmacia Biotech). The adsorbed fraction was eluted with a linear gradient consisting of 10 column volumes of 0 M to 1 M NaCl in 20 mM Tris-HCl buffer (pH 9.0). The fraction was dialyzed overnight against 20 mM CAPS-NaOH buffer (pH 10.0) at 4°C due to the formation of insoluble aggregates at neutral pH. The sample was applied to a HiTrap Q column equilibrated with 20 mM CAPS-NaOH buffer (pH 10.0). The adsorbed fraction was eluted with a gradient of 40 mM NaCl in 20 mM CAPS-NaOH buffer (pH 10.0). The homogeneity of the purified protein was confirmed by SDS-PAGE.

Purification of the β-Subunit—The dialyzed β-subunit was applied to a HiTrap Q column equipped with the ÄKTA FPLC system at 4°C equilibrated with 20 mM Tris-HCl buffer (pH 9.0). The adsorbed fraction was eluted with a linear gradient consisting of 10 column volumes of 0 M to 1 M NaCl in 20 mM Tris-HCl buffer (pH 9.0). The enzyme sample was dialyzed overnight against 20 mM HEPES-NaOH buffer (pH 9.0) at 4°C, and applied to a POROS HQ column (1 ml; Pharmacia Biotech) equilibrated with 20 mM HEPES-NaOH buffer (pH 9.0). The adsorbed fraction was eluted with a linear gradient consisting of 10 column volumes of 0 M to 1 M NaCl in 20 mM HEPES-NaOH buffer (pH 9.0). The purified solution was applied to a Superdex 200 HR column (24 ml; Pharmacia Biotech) equilibrated with 20 mM Tris-HCl buffer (pH 8.0) and 50 mM NaCl. The homogeneity of the purified protein was confirmed by SDS-PAGE.

Enzymatic Reaction of Tk-PheRS—The enzymatic activity of *Tk*-PheRS was estimated by the *N*-methylanthranioyl dATP (mdATP) method as described previously (*33*). The synthesized mdATP isolated by chromatography on a Sephadex LH-20 column (Pharmacia Biotech) was identified by a Perseptive Biosystems Mariner™ ESI-TOF MASS spectrometer (PerSeptive Biosystems, Framingham, MA) and ^{1}H NMR by a Varian Mercury 400 (400 MHz) spectrometer. The obtained mass of mdATP was 623.0454, which is almost identical to the calculated mass of 623.0457.

The sample was incubated at final concentration of 0.5 μM *Tk*-PheRS, 5 μM of mdATP, and 100 mM HEPES-NaOH buffer (pH 7.0) at 37°C for 30 min, and the fluorescence spectrum of the sample was monitored by excitation at 295 nm. When mdATP binds to *Tk*-PheRS, the fluorescence energy transfer (FRET) from the intrinsic tryptophan residues in *Tk*-PheRS to mdATP is detected by emission at around 445 nm. A substrate solution of 5 μM ATP and 5 μM Phe was added to the enzyme solution, and the decreased intensity at 445 nm with excitement at 295 nm was monitored at various temperatures from 20°C to 98°C using a Jasco fluorescence spectrometer, model FP6500, with a thermal control system (Japan Spectroscopic Company, Tokyo). The obtained curve was fitted to a single exponential equation and then the rate constant was determined at various temperatures.

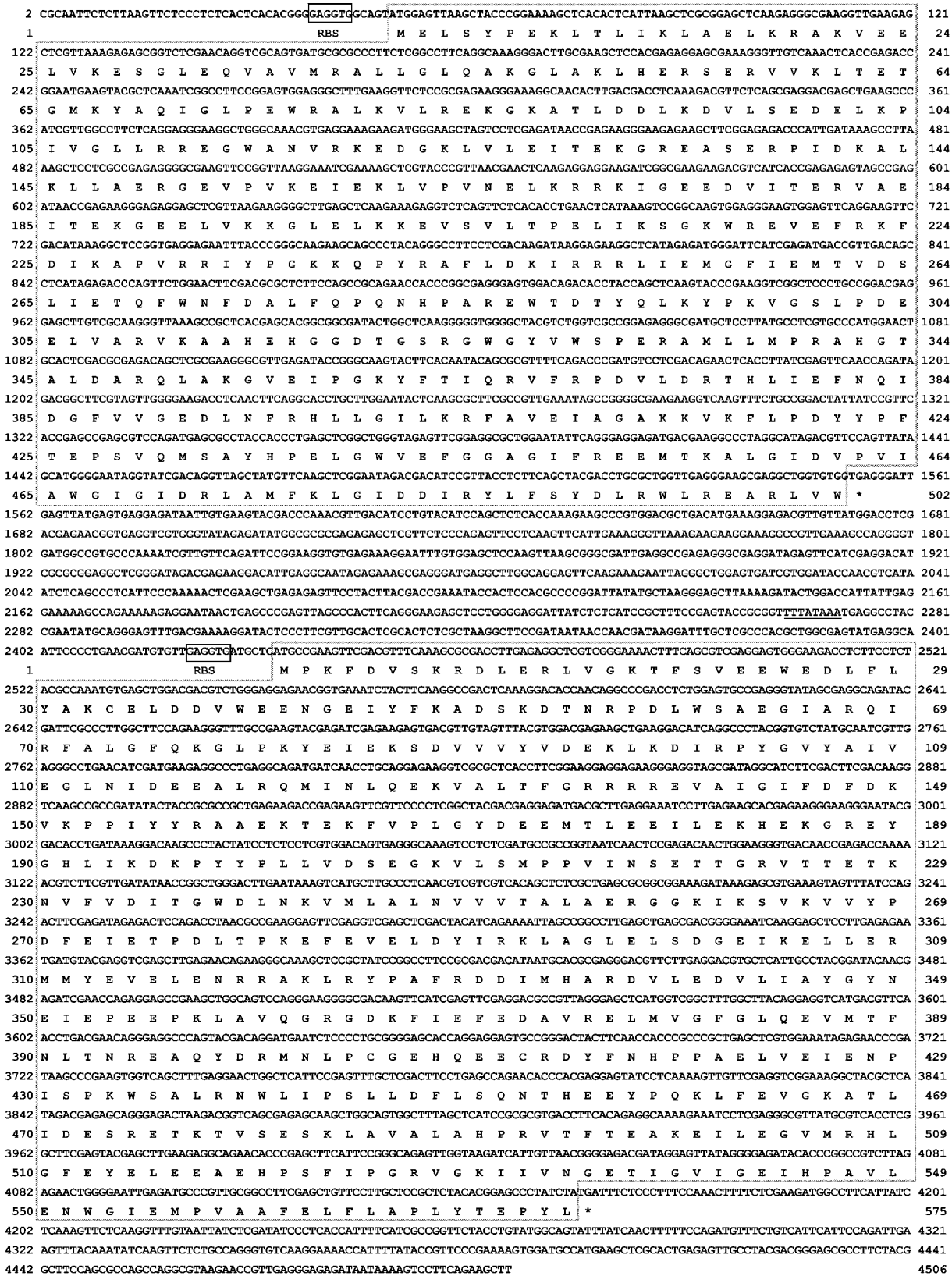

Fig. 1. **Nucleotide and deduced amino acid sequences of the *Tk-pheRSA* and *Tk-pheRSB* genes.** *Tk-pheRSA* and *Tk-pheRSB* are shown in the upper and lower squares, respectively. Ribosome binding sites (RBS) are indicated. A putative TATA box for *Tk-pheRSB* is underlined. Stop codons are indicated by asterisk.

```
Motif 1
    TKO 238    KQPYRAFLDKIRRRLIEMGEIEMTVDSLIETQFWNFDALFQPQNHPAREWTDTYQ
    MET 227    VHPLTRIIREVKEILLAMGFKEVKS PIVETETEFWNFDMLFEPQDHPARFMQDTFF
    TTH 100    LHPITLMERELVEIFRALGYQAVEG PEVESEFFNFDALNIPEHHPARDMWDTFW
    ECO 106    LHPVTRTIDRIESFFGELGFTVATG PEIEDDYHNFDALNIPGHHPARADHDTFW
    SCE 227    LHPLNKVREEFRQIFFSMGFTEMPSNQYVETGFWNFDALYVPQQHPARDLQDTFY
    HSA 224    LHPLLKVRSQFRQIFLEMGFTEMPTDNFIESSFWNFDALFQPQQHPARDQHDTFF

Motif 2                                                  Motif 3
    TKO 356    EIPGKYFTIQRVFRPDVLDRTHLIEFNQIDGFVV            TKO 461    VPVIAWGIGIDRLAMFKLGIDDIRY
    MET 340    NKPHKVFCIDRVFRNEAIDYKHLPEFYQCEGIIM            MET 444    KPVLAWGIGFSRLAMLRYGLTDIRD
    TTH 191    TPPFRIVVPGRVFRFEQTDATHEAVEHQLEGLVV            TTH 400    VTGFAFGLGVERLAMLRYGIPDIRY
    ECO 182    QPPIRIIAPGRVYRND YDQTHTPMEHQMEGLIV            ECO 290    YSGFAFGMGMERLTMLRYGVTDLRS
    SCE 347    PKPTRLFSIDRVFRNEAVDATHLAEFHQVEGVLA            SCE 454    LRVLGWGLSLERPTMIKYKVQNIRE
    HSA 345    FTPVKYFSIDRVFRNETLDATHLAEFHQIEGVVA            HSA 452    VSVIAWGLSLERPTMIKYGINNIRE
```

Fig. 2. **Amino acid alignment around the conserved motifs in pheRSA from archaea, bacteria, and eucarya.** TKO, *Thermococcus kodakaraensis*; MET, *Methanococcus jannaschii*; TTH, *Thermus thermophilus*; ECO, *Escherichia coli*; SCE, *Saccharomyces cerevisiae*; HSA, *Homo sapiens*. Bold underlined characters show amino acids that are identical in all sequences. Bold characters show amino acids with the same charges in all sequences or identical residues among 4–5 sequences. White letters on a black background show the catalytically important residues described in the text.

Circular Dichroism Spectra—Far-UV circular dichroism (CD) spectra were measured with a Jasco spectropolarimeter, model J-720W (Japan Spectroscopic Company), equipped with a thermal incubation system. The far-UV CD spectra of *Tk*-PheRS, α-subunit, and β-subunit were measured at protein concentrations of 0.1 mg/ml in 10 mM Tris-HCl buffer (pH 8.0) a 2 mm pathlength cell at 20°C. The thermal unfolding profile of *Tk*-PheRS was monitored by the CD intensity changes at 222 nm at a protein concentration of 0.14 mg/ml in 10 mM HEPES-NaOH buffer (pH 7.0). The rate of temperature increase was 1°C/min.

RESULTS AND DISCUSSION

Sequence analysis of the pheRS gene from T. kodakaraensis KOD1—Figure 1 shows the nucleotide and deduced amino acid sequences of the *pheRS* gene from *T. kodakaraensis* KOD1 (*Tk-pheRS*, GeneBank accession number AB093556). The open reading frames encoding the α- and β-subunits comprise 1,503 bases (501 amino acids) and 1,722 bases (574 amino acids), respectively. The molecular weight from the derived amino acid sequences of the α- and β-subunits are 57,600 and 66,200, respectively. The molecular weights of the α- and β-subunits from mesophilic bacteria (*E. coli*) are 37,300 and 87,400 (*34*); those from thermophilic bacteria (*T. thermophilus*) are 39,300 and 86,400 (*35*); those from eucarya (yeast) are 67,300 and 57,400 (*36*). Comparison of these values indicates that the masses of the subunits from KOD1 are similar to those from eucarya rather than those from bacteria.

Figure 2 shows the sequence alignments of the conserved class II motifs from archaea, eucarya, and bacteria. The putative catalytic site of the α-subunit is composed of conserved amino acid residues among class II

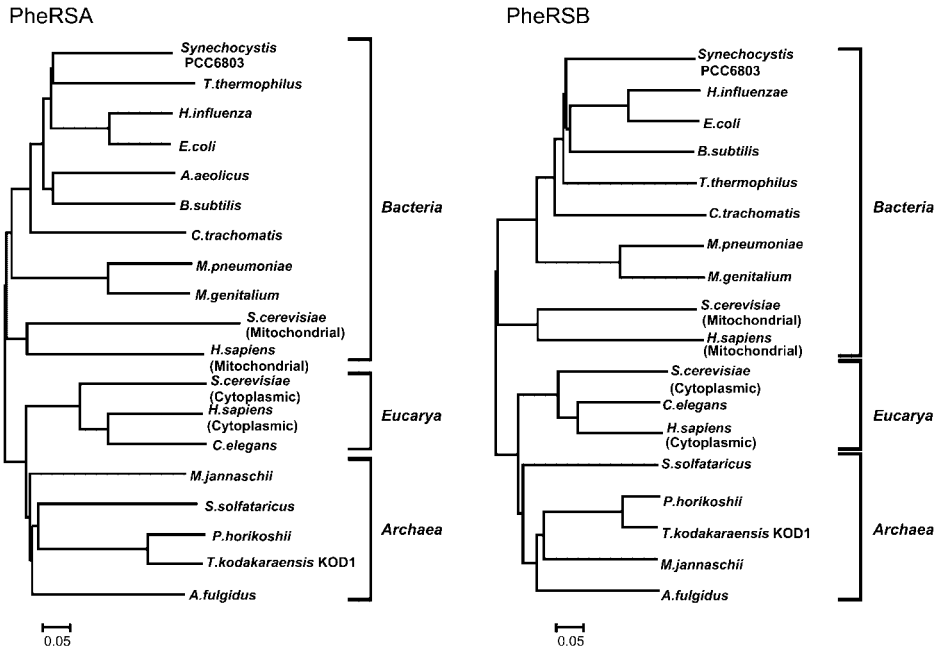

Fig. 3. **Phylogenetic relationship among 19 kinds of PheRSA and PheRSB.** Amino acid sequence alignment was carried out with the multiple alignment algorithm in Bioresearch/Sinca, version 2.0 (Fujitsu, Tokyo). The phylogenetic tree was constructed by the neighbor-joining method (*39*). The reliability of the tree nodes was analyzed by generating 1,000 bootstrap trees. The number of amino acid substitutions per site is shown by the scale.

Table 1. **Oligonucleotide distances between *pheRSA* and *pheRSB* genes.**

Species	Domain	Distance (bp)
Thermus thermophilus	Bacteria	0
Halobacterium sp. NRC-1	Archaea	0
Aeropyrum pernix	Archaea	1
Sulfolobus solfataricus	Archaea	5
Pyrococcus horikoshii	Archaea	11
Escherichia coli	Bacteria	14
Bacillus subtilis	Bacteria	15
Thermococcus kodakaraensis KOD1	Archaea	879
Pyrobaculum aerophilum	Archaea	121,701
Thermoplasma volcanium	Archaea	494,385
Methanococcus jannaschii	Archaea	616,437
Schizosaccharomyces pombe	Eucarya	911,749
Archaeoglobus fulgidus	Archaea	1,703,648
Methanosarcina mazei Goe1	Archaea	1,710,940
Methanosarcina acetivorans C2A	Archaea	2,302,929
Caenorhabditis elegans	Eucarya	chromosome 1 (α), 2 (β)
Saccharomyces cerevisiae	Eucarya	chromosome XII (α), VI (β)

aaRSs. The residues in motif 1 include an α-helix (residues Ile265-Asn280 in the α-subunit from KOD1) for the heterodimeric interface between the α- and β-subunits (*5*, *37*). Motifs 2 and 3 play crucial roles in the binding of the amino acid substrate and acceptor stem of the tRNA (*38*). Based on the crystal structure of *T. thermophilus*, catalytically important residues were identified for *Tk*-PheRSA. Phe391 in motif 2 and Arg472 in motif 3 bind to the adenosine moiety. Arg379 in motif 2 and Arg463 in motif 3 restrain the conformation with the triphosphate that interacts with the ribose hydroxyl and γ-phosphate. Asp395 in motif 2 is a unique residue; the position is Glu in other cases. Asp395 may bind to phenylalanine to assure proper positioning of the substrate.

Alignment of the amino acid sequences of the α- and β-subunits was based on pair-wise comparison. Figure 3 illustrates the phylogenetic relationship among PheRSs from various organisms using the Neighbor Jointing Method (*39*). The α- and β-subunits from KOD1 were grouped in the archaeal domain, with especially high similarity to *P. horikoshii* with a bootstrap value of 100%. The profiles of the tree for the α- and β-subunits agrees well with those of the universal tree based on 16S ribosomal RNA sequences (*40*).

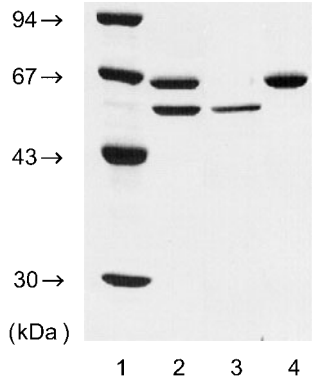

Fig. 4. **SDS-PAGE analysis of purified *Tk*-PheRS, *Tk*-PheRSA, and *Tk*-PheRSB.** Proteins were stained with Coomassie Brilliant Blue. 1, Standard markers; 2, *Tk*-PheRS; 3, *Tk*-PheRSA; 4, *Tk*-PheRSB.

A spacer region between the *Tk-pheRSA* (α-subunit) and *Tk-pheRSB* (β-subunit) genes is 879 bp, which is not necessarily a long spacer region compared with the genes from bacteria and four kinds of archaea (Table 1). On the other hand, the expression of these two genes might be controlled by their respective transcription units in the cases of encarya and other archaea, because there is a considerable distance between the two genes. Although *Tk-pheRSA* and *Tk-pheRSB* are clustered in the same direction and both locate at the same loci on the KOD1 chromosome, *Tk-pheRSB* possesses its own TATA box in the upstream region of the gene. Therefore, it was suggested that the *Tk-pheRSA* and *Tk-pheRSB* genes are transcribed independently in KOD1 cells, while both subunits are transcribed from the same promoter similar to the cases for bacterial PheRS genes (*41*).

Expression and Purification of Recombinant Tk-PheRS, Tk-PheRSA, and Tk-PheRSB—Recombinant proteins of *Tk*-PheRS and each subunit alone were expressed in *E. coli* cells. However, these proteins could not be expressed when *E. coli* BL21 (DE3) cells were used, probably due to the difference in codon usage between bacteria and archaea (*42*). *E. coli* BL21-CodonPlus (DE3)-RIL cells were successfully used for expression in all three cases. The cell extracts of the three expressed proteins were subjected to heat treatment at 80°C for 20 min, and crude extracts of the recombinant proteins were obtained in soluble fractions. After purification, the purity of each protein was evaluated by SDS-PAGE (Fig. 4). *Tk*-PheRS and the β-subunit were purified on a Superdex 200 column as the final step of protein purification. The purified *Tk*-PheRS and β-subunit chromatographed at ~250 kDa and ~130 kDa, indicating that *Tk*-PheRS and the β-subunit form $\alpha_2\beta_2$ and β_2 complexes, respectively.

Temperature Dependency of the Enzymatic Reaction—Activity measurements of *Tk*-PheRS were carried out using fluorescence energy transfer (FRET) from the intrinsic tryptophan to mdATP (*33*). The binding of mdATP to the active site of the protein leads to FRET due

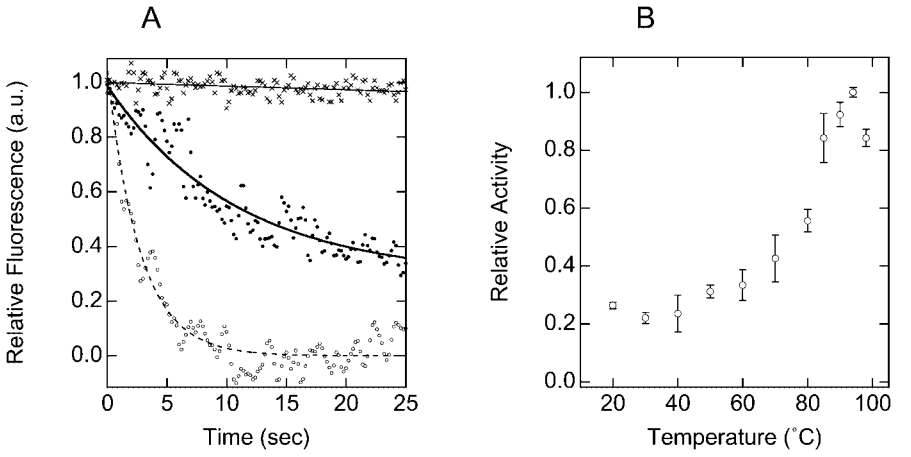

Fig. 5. **Estimated reaction of aminoacyl adenylate monitored by the mdATP method.** (A) Time-dependent displacement of mdATP by the synthesis reaction of aminoacyl adenylate. Activity was monitored at temperatures of 60°C (solid circles) and 98°C (open circles). As a control, instead of Phe and ATP, buffer was added and the activity was monitored at 60°C (crosses). The lines show the single-exponential fits to the data. (B) Temperature-dependent activity of the synthesis reaction of phenylalanine adenylate.

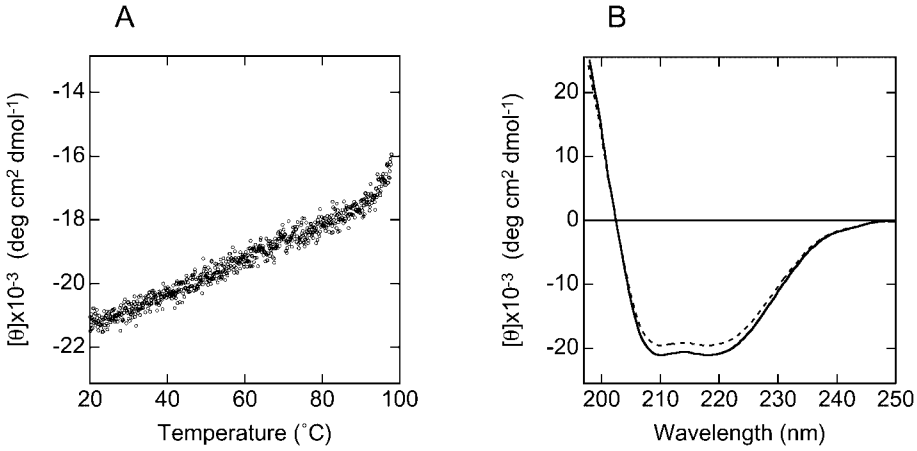

Fig. 6. **Thermal unfolding profile of *Tk*-PheRS as monitored by CD.** (A) Thermal unfolding profiles of *Tk*-PheRS monitored by the changes in CD intensity at 222 nm. (B) Far-UV CD spectra of *Tk*-PheRS at 20°C (continuous line) and at 90°C (dotted line).

to excited tryptophan fluorescence at 330–350 nm. The mdATP method is favorable for determining the temperature-dependent activity of aaRSs as compared with the conventional [γ-^{32}P]ATP method because the reaction can be directly monitored by fluorescence spectrometry. PheRS catalyzes the two reaction steps, ATP + Phe $\rightarrow$ AMP-Phe and AMP-Phe + tRNA $\rightarrow$ Phe-tRNA + AMP. The mdATP method detects the rate-limiting step of the former reaction. Figure 5 shows a temperature-dependent analysis of the synthesis reaction of *Tk*-PheRS. At 60°C and 98°C, the FRET intensity at 445 nm decreased upon the addition of ATP and Phe, however, the FRET intensity at 445 nm did not decrease by the addition of buffer at 60°C (Fig. 5A). The data were collected at 11 points between 20–98°C and the rate constants for the synthesis reaction were determined by single-exponential fitting (Fig. 5B). The enzymatic activity increased at higher temperatures. In particular, above 80°C, the activity increased rapidly. *Tk*-PheRS showed maximum activity at around 95°C.

Thermal Unfolding Profile of Tk-PheRS—Figure 6 shows thermal unfolding profiles of *Tk*-PheRS as monitored by the CD intensity changes at 222 nm. With increasing temperature, the intensity of the far-UV CD signal decreased slightly (Fig. 6A). The secondary structure was retained below 95°C (Fig. 6B). With further increasing temperature, the CD intensity decreased steeply, which corresponds to the thermal unfolding signal. PheRS from *E. coli* is inactivated by heat treatment at 43°C (*43*); after heat treatment for 10 min, the temperature for the half-time inactivation of PheRS from the archaeal *Sulfolobus solfataricus* is estimated to be 88°C (*44*). On the other hand, *Tk*-PheRS retains its activity and tertiary structure at 95°C, indicating that *Tk*-PheRS is the most thermostable PheRSs reported.

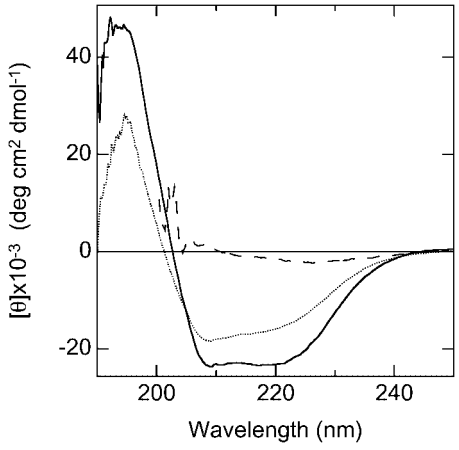

Fig. 7. **Far-UV CD spectra of *Tk*-PheRS, *Tk*-PheRSA, and *Tk*-PheRSB.** Far-UV CD spectra of *Tk*-PheRS (continuous line), α-subunit alone (broken line), and β-subunit alone (dotted line) were measured at 20°C.

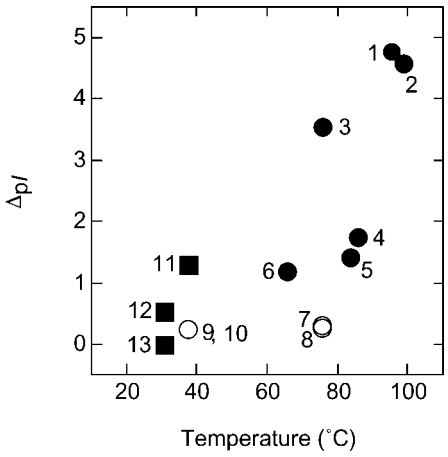

Fig. 8. **Relationship between the difference of the isoelectric point of each subunit (Δp*I*) and growth temperature of the organism.** Δp*I* values of PheRSs from archaea, bacteria, and eucarya are shown as solid circles, open circles, and closed squares, respectively. 1, *T. kodakaraensis*; 2, *P. horikoshii*; 3, *S. solfataricus*; 4, *M. jannaschii*; 5, *A. fulgidus*; 6, *M. thermoautotorophicum*; 7, *T. aquaticus*; 8, *T. thermophilus*; 9, *B. subtilis*; 10, *E. coli*; 11, *H. sapiens*; 12, *S. cerevisiae*; 13, *C. elegans*.

CD Analyses of Tk-PheRS, and Its α- and β-Subunits—Figure 7 shows far-UV CD spectra of *Tk*-PheRS, the α-subunit, and the β-subunit. *Tk*-PheRS possesses high α-helical content as indicated by a typical α-helical far-UV CD spectrum with characteristic peaks at 222 nm and 208 nm. The α-subunit does not form any definite secondary structure. On the other hand, the β-subunit shows a typical α-helical structure in the far-UV CD spectrum. The purified β-subunit forms dimers as judged by gel-filtration analysis (data not shown), while the purified α-subunit is prone to form aggregates at neutral pH. These data imply that the formation of the oligomeric interfaces of *Tk*-PheRS is arranged in the order of α-β-β-α, which is conserved in PheRSs from archaea and eucarya.

Structural Implications for an Archaeal PheRS—*Tk*-PheRS is very thermostable with an optimum temperature for activity at 95°C, which is the most thermostable aaRSs reported. The difference in the isoelectric points (Δp*I*) between the α-subunit (p*I* = 9.39) and β-subunit (p*I* = 4.62) might be significant in facilitating the interaction between these two subunits and in maintaining the thermostable structure of PheRS. Figure 8 shows the Δp*I* between the α- and β-subunits plotted against the growth temperatures of the organisms. The Δp*I* clearly increases as the growth temperature increases, indicating the importance of the electrostatic interaction for adaptation to high temperatures. In fact, hyperthermophilic proteins possess large numbers of ion-pairs or ion-pair networks on their surface and at protein–protein interfaces (*45–47*). While it is unclear whether the electrostatic interaction is the major factor for protein interactions (*48*), the clear relationship shown in Fig. 8 implies that the electrostatic interaction between the α- and β-subunits plays an important role in facilitating and retaining the tetrameric $\alpha_2\beta_2$ structure at high temperatures. These implications provide basic information about the uniqueness of PheRS as well as protein-protein interactions in hyperthermophilic proteins that allow them to retain their tertiary structures at growth temperature above 90°C.

This work was supported by a Grant-in-Aid for Scientific Research from the Ministry of Education, Science, Sports and Culture of Japan (14350433, 14045229) and a grant from the Science and Technology Incubation Program in Advanced Region by JST (Japan Science and Technology Corporation).

REFERENCES

1. Jakubowski, H. and Goldman, E. (1992) Editing of errors in selection of amino acids for protein synthesis. *Microbiol. Rev.* **56**, 412–429
2. Giegé, R., Sissler, M., and Florentz, C. (1998) Universal rules and idiosyncratic features in tRNA identity. *Nucleic Acids Res.* **26**, 5017–5035
3. Wolf, Y.I., Aravind, L., Grishin, N.Y., and Koonin, E.V. (1999) Evolution of aminoacyl-tRNA synthetases-analysis of unique domain architectures and phylogenetic trees reveals a complex history of horizontal gene transfer events. *Genome Res.* **8**, 689–710
4. Woese, C.R., Olsen, G.J., Ibba, M., and Soll, D. (2000) Aminoacyl-tRNA synthetases, the genetic code, and the evolutionary process. *Microbiol. Rev.* **64**, 202–236
5. Eriani, G., Delarue, M., Poch, O., Gangloff, J., and Moras, D. (1990) Partition of tRNA synthetases into two classes based on mutually exclusive sets of sequence motifs. *Nature* **347**, 203–206
6. Brick, P., Bhat, T.N., and Blow, D.M. (1988) Structure of tyrosyl-tRNA synthetase refined at 2.3 Å resolution. Interaction of the enzyme with the tyrosyl-adenylate intermediate. *J. Mol. Biol.* **208**, 83–98
7. Rould, M.A., Perona, J.J., Soll, D., and Steitz, T.A. (1989) Structure of *E. coli* glutaminyl-tRNA synthetase complexed with tRNAGln and ATP at 2.8 Å Rresolution. *Science* **246**, 1135–1142
8. Brunie, S., Zelwer, C., and Risler, J.L. (1990) Crsytallographic study at 2.5 Å resolution of the interaction of methionyl-tRNA synthetase from *Escherichia coli* with ATP. *J. Mol. Biol.* **216**, 411–424
9. Doublie, S., Bricogne, G., Gilmore, C., and Carter, C.W. (1995) Tryptophanyl-tRNA synthetase crystal structure reveals an unexpected homology to tyrosyl-tRNA synthetase. *Structure* **3**, 17–31
10. Nureki, O., Vassylyev, D.G., Katayanagi, K., Shimizu, T., Sekine, S., Kigawa, T., Miyazawa, T., Yokoyama, S., and Morikawa, K. (1995) Architectures of class-defining and specific domains of glutamyl-tRNA synthetase. *Science* **267**, 1958–1965
11. Silvian, L.F., Wang, J., and Steitz, T.A. (1999) Insights into editing from an Ile-tRNA synthetase structure with $tRNA^{ile}$ and mupirocin. *Science* **285**, 1074–1077
12. Cavarelli, J., Eriani, G., Rees, B., Ruff, M., Boeglin, M., Mitschler, A., Martin, F., Gangloff, J., Thierry, J.C., and Moras, D. (1994) The active site of yeast aspartyl-tRNA synthetase: structural and functional aspects of the aminoacylation reaction. *EMBO J.* **13**, 327–337
13. Cusack, S., Berthet-Colominas, C., Hartlein, M., Nassar, N., and Leberman, R. (1990) A 2nd class of synthetase structure revealed by X-ray analysis of *Escherichia coli* seryl-transfer RNA synthetase at 2.5 Å. *Nature* **347**, 249–255
14. Ruff, M., Boeglin, A.M., Poterszman, A., Podjarny, A., Mitschler, A., Rees, B., Thierry, J.C., and Moras, D. (1991) Class II aminoacyl transfer RNA synthetases: Crystal structure of yeast aspartyl-tRNA synthetase complexed with $tRNA^{Asp}$. *Science* **252**, 1682–1689
15. Onesti, S., Miller, A.D., and Brick, P. (1995) The crystal structure of the lysyl-tRNA synthetase (LysU) from *Escherichia coli*. *Structure* **3**, 163–176

16. Logan, D.T., Mazauric, M.H., Kern, D., and Moras, D. (1995) Crystal structure of glycyl-tRNA synthetase from *Thermus thermophilus*. *EMBO J.* **14**, 4156–4167
17. Goldgur, Y., Mosyak, L., Reshetnikova, L., Ankilova, V., Lavrik, O., Khodyreva, S., and Safro, M. (1997) The crystal structure of phenylalanyl-tRNA synthetase from *Thermus thermophilus* complexed with cognate $tRNA^{Phe}$. *Structure* **5**, 59–68
18. Cusack, S., Yaremchuk, A., Krikliviy, I., and Tukalo, M. (1998) $tRNA^{Pro}$ anticodon recognition by *Thermus thermophilus* prolyl-tRNA synthetase. *Structure* **6**, 101–108
19. Berthet-Colominas, C., Seignovert, L., Hartlein, M., Grotli, M., Cusack, S., and Leberman, R. (1998) The crystal structure of asparaginyl-tRNA synthetase from *Thermus thermophilus* and its complexes with ATP and asparaginyl-adenylate: the mechanism of discrimination between asparagine and aspartic acid. *EMBO J.* **17**, 2947–2960
20. Mosyak, L., Reshetnikova, L., Goldgur, Y., Delarue, M., and Safro, M.G. (1995) Structure of phenylalanyl-tRNA synthetase from *Thermus thermophilus*. *Nat. Struct. Biol.* **2**, 537–547
21. Keller, B., Kast, P., and Hennecke, H. (1992) Cloning and sequence analysis of the phenylalanyl-tRNA synthetase genes (pheST) from *Thermus thermophilus*. *FEBS Lett.* **301**, 83–88
22. Savopoulos, J.W., Hibbs, M., Jones, E.J., Mensah, L., Richardson, C., Fosberry, A., Downes, R., Fox, S.G., Brown, J.R., and Jenkins, O. (2001) Identification, cloning, and expression of a functional phenylalanyl-tRNA synthetase (pheRS) from *Staphylococcus aureus*. *Protein. Expr. Purif.* **21**, 470–484
23. Hountondji, C., Schmitter, J.M., Beauvallet, C., and Blanquet, S. (1987) Affinity labeling of *Escherichia coli* phenylalanyl-tRNA synthetase at the binding site for $tRNA^{Phe}$. *Biochemistry* **26**, 5433–5439
24. Roth, A., Eriani, G., Dirheimer, G., and Gangloff, J. (1993) Kinetic properties of pure overproduced *Bacillus subtilis* phenylalanyl-tRNA synthetase do not favor its *in vivo* inhibition by ochratoxin A. *FEBS Lett.* **326**, 87–91
25. Savopoulos, J.W., Hobbs, M., Jones, E.J., Mensah, L., Richardson, C., Fosberry, A., Downes, R., Fox, S.G., Brown, J.R., and Jenkins, O. (2001) Identification, cloning, and expression of a functional phenylalanyl-tRNA synthetase (pheRS) from *Staphylococcus aureus*. *Protein Exp. Purif.* **21**, 470–484
26. Bullard, J.M., Cai, Y.C., Demeler, B.L., and Spremulli, L. (1999) Expression and characterization of a human mitochondrial phenylalanyl-tRNA synthetase. *J. Mol. Biol.* **288**, 567–577
27. Rauhut, R., Gabius, H.J., Kuhn, W., and Cramer, F. (1984) Phenylalanyl-tRNA synthetase from the archaebacterium *Methanosarcinabarkeri*. *J. Biol. Chem.* **259**, 6340–6345
28. Das, R. and Vothknecht, U.C. (1999) Phenylalanyl-tRNA synthetase from the archaeon *Methanobacterium thermoautotrophicum* is an $(\alpha\beta)_2$ heterotetrameric protein. *Biochimie* **81**, 1037–1039
29. Morikawa, M., Rashid, Y.N., Hoaki, T., and Imanaka, T. (1994) Purification and characterization of a thermostable thiol protease from a newly isolated hyperthermophilic *Pyrococcus* sp. *Appl. Environ. Microbiol.* **60**, 4559–4566
30. Imanaka, T., Lee, S., Takagi, M., and Fujiwara, S. (1995) Aspartyl-tRNA synthetase of the hyperthermophilic archaeon *Pyrococcus* sp. KOD1 has a chimerical structure of eukaryotic and bacterial enzymes. *Gene* **164**, 153–156
31. Fujiwara, S., Lee, S.G., Haruki, M., Kanaya, S., Takagi, M., and Imanaka, T. (1996) Unusual enzyme characteristics of aspartyl-tRNA synthetase from hyperthermophilic archaeon *Pyrococcus* sp. KOD1. *FEBS Lett.* **394**, 66–70
32. Schmitt, E., Moulinier, L., Fujiwara, S., Imanaka, T., Thierry, J.-C., and Moras, D. (1998) Crystal structure of aspartyl-tRNA synthetase from *Pyrococcus kodakaraensis* KOD: archaeon specificity and catalytic mechanism of adenylate formation. *EMBO J.* **17**, 5227–5237
33. Nomanbhoy, T.K. and Schimmel, P. (2001) Active site of an aminoacyl-tRNA synthetase dissected by energy-transfer-dependent fluorescence. *Bioorg. Med. Chem. Lett.* **11**, 1485–1491
34. Fayat, G., Mayaux, J.F., Sacerot, C., Springer, M., Fromant, M., Grunberg-Manago, M., and Blanquet, S. (1983) *Escherichia coli* phenylalanyl-tRNA synthetase operon region. Evidence for an attenuation mechanism. Identification of the gene for the ribosomal protein L20. *J. Mol. Biol.* **171**, 239–261
35. Mechulam, Y., Fayat, G., and Blanquet, S. (1985) Sequence of the *Escherichia coli* pheST operon and identification of the *himA* gene. *J. Bacteriol.* **163**, 787–791
36. Sanni, A., Mirande, M., Ebel, J.P., Boulanger, Y., Waller, J.P., and Fasiolo, F. (1988) Structure and expression of the genes encoding the α- and β-subunits of yeast phenylalanyl-tRNA synthetase. *J. Biol. Chem.* **263**, 15407–15415
37. Cusack, S. (1997) Aminoacyl-tRNA synthetases. *Curr. Opin. Struct. Biol.* **7**, 881–889
38. Reshetnikova, L., Moor, N., Lavrik, O., and Vassylyev, D.G. (1999) Crystal structures of phenylalanyl-tRNA synthetase complexed with phenylalanine and a phenylalanyl-adenylate analogue. *J. Mol. Biol.* **287**, 555–568
39. Saito, H. and Nei, M. (1987) The neighbor-joining methods: A new method for reconstructing phylogenetic trees. *Mol. Biol. Evol.* **4**, 406–425
40. Woese, C.R. (1987) Bacterial evolution. *Bicrobiol. Rev.* **51**, 221–271
41. Plumbridge, J.A. and Springer, M. (1980) Gene for the two subunits of phenylalanyl-tRNA snthetase of *Escherichia coli* are transcribed from the same promoter. *J. Mol. Biol.* **144**, 595–600
42. Hashimoto, Y., Yamamoto, T., Fujiwara, S., Takagi, M., and Imanaka, T. (2001) Extracellular synthesis, specific recognition, and intracellular degradation of cyclomaltodextrins by the hyperthermophilic archaeon *Thermococcus* sp. strain B1001. *J .Bacteriol.* **183**, 5050–5057
43. Bobkova, E.V., Stepanov, V.G., and Lavrik, O.I. (1992) A comparative study of the relationship between thermostability and function of phenylalanyl-tRNA synthetases from *Escherichia coli* and *Thermus thermophilus*. *FEBS Lett.* **302**, 54–56
44. Lombardo, B., Raimo, G., and Bocchini, V. (2002) Molecular and functional properties of an archaeal phenylalanyl-tRNA synthetase from the hyperthermophile *Sulfolobus solfataricus*. *Biochim. Biophys. Acta* **1596**, 246–252
45. Rice, D.W., Yip, K.S.P., Stillman, T.J., Britton, K.L., Fuentes, A., Connerton, I., Pasquo, A., Scandurra, R., and Engel, P.C. (1996) Insights into the molecular basis of thermal stability from the structure determination of *Pyrococcus furiosus* glutamate dehydrogenase. *FEMS Microbiol. Rev.* **18**, 105–117
46. Britton, K.L., Yip, K.S., Sedelnikova, S.E., Stillman, T.J., Adams, M.W., Ma, K., Maeder, D.L., Robb, F.T., Tolliday, N., Vetriani, C., Rice, D.W., and Baker, P.J. (1999) Structure determination of the glutamate dehydrogenase from the hyperthermophile *Thermococcus litralis* and its comparison with that from *Pyrococcus furiosus*. *J. Mol. Biol.* **293**, 1121–1132
47. Hashimoto, H., Inoue, T., Nishioka, M., Fujiwara, S., Takagi, M., Imanaka, T., and Kai, Y. (1999) Hyperthermostable protein structure maintained by intra- and inter- helix ion-pairs in archaeal O^6-methylguanine-DNA methyltransferase. *J. Mol. Biol.* **292**, 707–716
48. Kumar, S. and Nussinov, R. (1999) Salt bridge stability in monomeric proteins. *J. Mol. Biol.* **293**, 1241–1255